Comprehensive two-dimensional liquid chromatography – high-resolution mass spectrometry for complex protein digest analysis using parallel gradients

Rick S. van den Hurk [a,b], Bart Lagerwaard [a,b], Nathan J. Terlouw [a,b], Mingzhe Sun [a,b], Job J. Tieleman [a,b], Anniek X. Verstegen [a,b], Saer Samanipour [a,b], Bob W.J. Pirok [a,b] , Andrea F.G. Gargano [a,b*]

[a] *Analytical Chemistry Group, Van 't Hoff Institute for Molecular Sciences, University of Amsterdam, The Netherlands*

[b] *Centre for Analytical Sciences Amsterdam (CASA), the Netherlands*

* Corresponding author

Andrea F.G. Gargano a.gargano@uva.nl

Keywords: two-dimensional liquid chromatography, parallel gradients, shifted gradients, protein digest analysis, high-resolution mass spectrometry

Abstract

Despite the high gain in peak capacity, online comprehensive two-dimensional liquid chromatography coupled with high-resolution mass spectrometry (LC×LC-HRMS) has not yet been widely applied to the analysis of complex protein digests. One reason is the methods' reduced sensitivity that can be linked to the high flow rates of the second separation dimension (^{2}D). This results in higher dilution factors and the need for flow splitters to couple to ESI-MS.

This study reports proof of principle results of the development of an RPLC×RPLC-HRMS using parallel-gradients (^{2}D flow rate of 0.7 mL min^{-1}) and its comparison to shifted gradient methods (^{2}D of 1.4 mL min^{-1}) for the analysis of complex digests using a QExactive-Plus MS. Shifted and parallel-gradients resulted in high surface coverage (SC) and effective peak capacity (SC of 0.6226 and 0.7439 and an effective peak capacity of 779 and 757 in 60 minutes). When applied to a cell line digest sample, parallel-gradients allowed higher sensitivity (e.g., average MS intensity increased by a factor of 3), allowing for a higher number of identifications (e.g., about 2600 vs 3900 peptides). In addition, reducing the modulation time to 10s significantly increased the number of MS/MS events that could be performed. When compared to a 1D-RPLC method, parallel RPLC×RPLC-HRMS methods offered higher separation performance (FHWH from 0.12 to 0.018 min) with limited sensitivity losses resulting in an increase of analyte identifications (e.g. about 6000 vs 7000 peptides).

1. Introduction

Modern liquid chromatography (LC) high-resolution mass spectrometry (HRMS) instruments reach scan rates of over 50 Hz allowing for fast analysis and fragmentation experiments. This

makes LC-HRMS the method of choice to study changes in the proteome of complex organisms and to characterize the sequence of proteins, such as biotherapeutics. [1–3]. In these experiments, proteins are digested into peptides and LC separations are essential to resolve the tens of thousands of peptides in a sample. [4] The separation quality thus significantly influences the speed and depth of this analysis.[5] The metric most often used to describe the quality of an LC separation is the peak capacity, approximating the maximum number of peaks that can be resolved at an equal resolution within a given separation space.[6] Ultra-high-pressure LC technology commonly allows for peak capacity between 100 and 200 per hour.[7] For the analysis of highly complex samples, comprehensive two-dimensional LC (LC×LC) is an attractive option as it can offer one order of magnitude higher peak capacity.[8–11]

In the past years, LC×LC has been applied for separating protein digests or other peptide mixtures. A commonly applied selectivity combination is RPLC×RPLC.[12] This combination yields fundamentally limited orthogonality yet provides excellent solvent compatibility between the dimensions and high-resolution separations. The most common methods either employ different column chemistries (*e.g.* [13]) or combine basic mobile phases in the first dimension (^{1}D) with acidic RPLC in the second dimension (^{2}D; e.g. [4]). Nevertheless, the limited orthogonality of the two methods results in low retention-space utilization when using full-gradients (the same gradient in every ^{2}D separation, e.g. 2-45%B). For this reason, shifted gradients (the lower and upper boundary of the ^{2}D gradient change) can be used where the ^{2}D mobile phase gradient method is correlated to the gradient program in ^{1}D to maximize the surface coverage [9]. Using this approach, Stoll *et al.* reached a peak capacity of 10,000 in 4 hrs for the analysis of a monoclonal antibody digest [4]. Despite high-performance, the use of shifted gradients has also been criticized. Chapel *et al.* [14] found that the increase in retention space coverage and peak capacity is obtained at the expense of sensitivity and retention time repeatability in consecutive ^{2}D separations.

Moreover, the most critical disadvantage of any repeating gradient (i.e. shifted or full) in RPLC×RPLC is that high flow rates (>1 mL min^{-1}) are required to minimize dwell time, column equilibration time, and t0 along with increasing the normalized gradient slope and overall separation power. However, high flow rates increase the dilution factors and require the use of post-column flow splitting to allow for hyphenation with MS, inducing band distortion and losses in sensitivity.[15]

One alternative to shifted gradients to extend the usage of the ^{2}D retention space in RPLC×RPLC is using parallel-gradients. With this approach, in the second-dimension separation, a single gradient with a slope correlated to the first dimension (hence "parallel") is programmed throughout the analysis. Parallel-gradients have been investigated since 2003[16], demonstrating that this method can improve the use of available ^{2}D separation space in correlated RPLC×RPLC platforms.[17–20] An additional advantage is that a more constant pressure on the ^{2}D column, reducing physical stress on the column and other system components.[21] Moreover, parallel-gradients do not require high ^{2}D flow rates and consequently omit the need for post-column flow splitting when hyphenating to MS. Various applications have been demonstrated with these method, such as pharmaceuticals analysis[22], food[23,24], and simple aromatic compounds.[29]

In this work, we developed a parallel-gradients RPLC×RPLC method for peptide separations and compared it to full- and shifted-gradients. All methods employed stationary-phase-assisted modulation (SPAM) as a modulation strategy.[25–27] Our comparison was based on the effective peak capacity, sensitivity, surface coverage, and repeatability. Finally, the methods were evaluated based on their protein-identification capacity by measuring a cell lysate using MS/MS. Shorter modulation times for parallel-gradient methods were also explored.

2. Experimental

2.1 Chemicals

Water (ULC/MS grade) and acetonitrile (ACN, LC-MS grade) were obtained from Biosolve (Valkenswaard, The Netherlands). Dichloromethane (DCM) was obtained from VWR chemicals (Fontenay-sous-Bois, France). Ammonium bicarbonate (Bioultra, ≥ 99.5%) was acquired from Fluka Analytical (Charlotte, USA). Formic acid (FA, ≥98%) and Ammonium formate (AmFm) were obtained from Sigma (Zwijndrecht, The Netherlands). The ammonium hydroxide solution was obtained from Thermoscientific (The Netherlands).

Alpha casein (≥ 70.0%), bovine serum albumin (BSA, lyophilised powder, ≥ 96%), myoglobin (from equine heart, essentially salt-free, lyophylized powder, ≥ 90% (SDS-PAGE)), albumin (from chicken egg white, lyophilized powder, ≥98%, agarose gel electrophoresis), urea (≥ 98%), trypsin (BRP grade), thiourea (puriss. p.a., ACS reagent, ≥ 99.0%), were all obtained from Sigma (Zwijndrecht, The Netherlands). Human IMR90 lung fibroblast cells (ATCC CCL-186) were prepared according to what was described in [28]. Solid-phase extraction (SPE) was performed with C18 cartridges (Supelco; 1 mL, 100 mg bed, pore size 70 Å)

2.2 Instrumentation

All experiments in this study were carried out using an Agilent 1290 series Infinity 2D-LC system (Agilent, Waldbronn, Germany). The system comprised of two binary Infinity I pumps (G4220A), one 1100 isocratic pump (G1310A), an autosampler (G4226A), a thermostatted column compartment (G1316C), a valve drive (G1170A), equipped with an 8-port 2-position 2D-LC valve (G4236A), and a diode-array detector (G4212A) with Agilent Max-Light cartridge cells (G4212-60008, 10 mm, detector volume = 1.0 µL). The system was controlled using Agilent OpenLAB CDS Chemstation Edition (Version 3.2 (Build 3.2.0.620)) software.

The ^{1}D columns were Agilent InfinityLab Poroshell 120 HPH-C18 (150×2.1mm, 1.9 µm), Agilent ZORBAX SB-CN and Agilent ZORBAX Eclipse Plus C18 (both 150×2.1mm, 1.8 µm). The ^{2}D column was a ZORBAX Eclipse Plus C18 (50×2.1mm, 1.8 µm). In addition, an Agilent ZORBAX SB-CN (50×2.1mm, 1.8 µm) and an Agilent InfinityLab Poroshell 120 HPH-C18 (50×2.1mm, 1.9 µm) were used.

To perform SPAM in the 2DLC experiments, two Phenomenex SecurityGuard™ ULTRA C18 Cartridges (2×2.1mm) were used with the corresponding Phenomenex SecurityGuard™ ULTRA Holders. The mass spectrometer used was a Q-Exactive-Plus (Thermo Scientific, Bremen, Germany).

2.3 Procedures

2.3.1 Sample preparation

A protein digest sample consisting of BSA or four different proteins (BSA, ***α***-casein, myoglobin, and albumin) was used for method development. A cell lysate (human IMR90 lung fibroblast cells) was used to prove the method's applicability. The sample preparation is based on previously described work.[29]Details on procedures are described in the Supporting Information (SI) Section S-1.

2.3.2 1DLC-HRMS

For all 1D-LC experiments, the column was directly connected to the MS source. The injection volume was 2 µL, and the column thermostat was 50 °C. Mobile phase A consisted of H_2O, mobile phase B was ACN. To both mobile phases, 0.1% FA was added with the exception of the mobile phase used for the HPH-C18 column. For the high-pH separations, A was H_2O with 20 mM AmFm at pH 10 (adjusted using ammonium) and B was plain ACN. A full overview of the used MS settings is presented in the SI Section S-2.

To compare 1D-LC with 2D-LC, 1D-LC a 150×2.1mm column, a flow rate of 0.16 mL min^{-1} and a gradient from 2-38%B in 60 minutes. The exact gradient programming for all of these experiments can be found in the SI Section S-3.

2.3.3 RPLC×RPLC-HRMS

Sample, solvent composition (of both ^{1}D and ^{2}D separations), column temperature and MS settings were the same as described in the previous section. For the 2D-LC experiments, the ^{1}D column was 150mm in length and the HPH-C18 for full and shifted gradients while the CN was used for parallel-gradients and the ^{2}D column was C18. A schematic overview of the system is depicted in Figure S1 in the SI. 2 µL of sample was injected for the protein mix and 15 uL for the cell lysate. In all cases where the ^{1}D flow rate was 0.16 mL min^{-1}, the ^{1}D gradient for the HPH-C18 column was programmed in the following steps: 0-60-65-70-70.01 min and respectively 2-38-90-90-2 for the percentage of B. For the CN column, the third step was reduced from 38% B to 32% B. For all methods, a modulation time of 30 seconds was used. For SPAM, a dilution ratio of 1:3 (water 0.1%FA) was applied (0.48 mL min^{-1}).

The full-gradient and shifted-gradient methods used the HPH-C18 column and solvents in the first dimension and the 50mm C18 in the second dimension at a flow rate of 1.4 mL min^{-1} and a 1:1 ratio flow split prior to the MS. The full-gradient method employed a linear solvent gradient from 2-45% B in every modulation over the first 0.43 min followed by 0.07 min equilibration at 2% B. The detailed shited gradient programming can be found in Section S-4.

For the parallel gradient, the 150mm CN column was used for the ^{1}D. The ^{2}D gradient was programmed in the following steps: 0-60-65-70-70.01 min and respectively 12-40-90-90-12 for the percentage of B. Contrary to the other methods, the ^{2}D flow rate was set at 0.7 mL min^{-1} and therefore without the use of a flow splitter.

2.3.4 MS conditions and Data handling

MS data were recorded using a HESI source. A full overview of the used MS settings is presented in the SI Section S-2. Plotting of the 2DLC chromatograms and other calculations were performed using MATLAB R2024a. For the equations used to calculate several parameters, the reader is referred to SI Section S-5. MZmine version 3.90 was used for feature detection from LC and LC×LC-MS experiments[30]. Peptide and protein identification was performed in MaxQuant (V2.1). Carbamidomethyl was used as a fixed modification and the variable modifications were set to oxidation and acetylation. Trypsin was specified as the enzyme, with a maximum of two missed cleavages. The false discovery rate (FDR) for the peptide identification was set to 1%. Further details can be found in the SI Section S-6 Raw data and MaxQuant analysis results are available at https://massive.ucsd.edu/ProteoSAFe dataset MSV000094598.

3. Results and Discussion

Here, we describe the development of a parallel-gradient LC×LC method based on RPLC separations on both dimensions and compare (in section 3.3) it to a full and a shifted-gradient method similar to previous research.[4]

3.1 Screening of ^{1}D selectivities

To effectively use the 2DLC separation space in LC×LC separations using full-gradient programs the two coupled methods should have the highest orthogonality (lowest correlation) possible. In contrast, for shifted and parallel-gradient methods, the two separation dimensions must be correlated but feature different selectivities (e.g., different elution order of analytes).[22,24] Therefore, to establish a parallel RPLC×RPLC method, we initially screened several RPLC peptide separation methods (see supporting information S-7). We then selected

three RPLC methods (using 150×2.1 mm ID columns) and measured the correlation between the LC-MS separation of a trypsin digest of a mixture of four proteins (BSA, $\boldsymbol{\alpha}$-casein, myoglobin and albumin). All the methods used ACN as organic modifier, low-pH C18 (LPH) and cyano (CN) using 0.1% FA and high-pH C18 (HPH) using a 20 mM AmFm at pH 10. To evaluate the results, we used the R^2-value from a linear trendline of the normalized analyte retention time (ntr, calculated as $(t_{r,i}-t_{r,first})/(t_{r,last}-t_{r,first})$) of a specific analyte for each LC separation (Figure 1). Lower R^2-value represents lower correlation and therefore, higher orthogonality of the compared selectivities. The lowest correlation ($R^2 = 0.711$) was observed between the LPH and HPH whereas the correlation between the LPH and CN (at the same pH) was significantly higher ($R^2 = 0.933$). This is likely to occur due to the changes in the charge of peptides between the different pH environments of HPH and LPH separations. Although this condition is generally considered beneficial for 2DLC methods, this is not the case for parallel-gradients, as large differences in retention may lead to part of the compounds not eluting within the modulation time (wrap-around) or having significantly wider peak widths due to high retention or eluting unretained. Because of the high correlation but sufficient differences observed in the analyte elution order, we used the CN×LPH combination to develop a parallel-gradient RPLC×RPLC. In the case of shifting gradients, the HPH×LPH was used following what was reported by. [4]

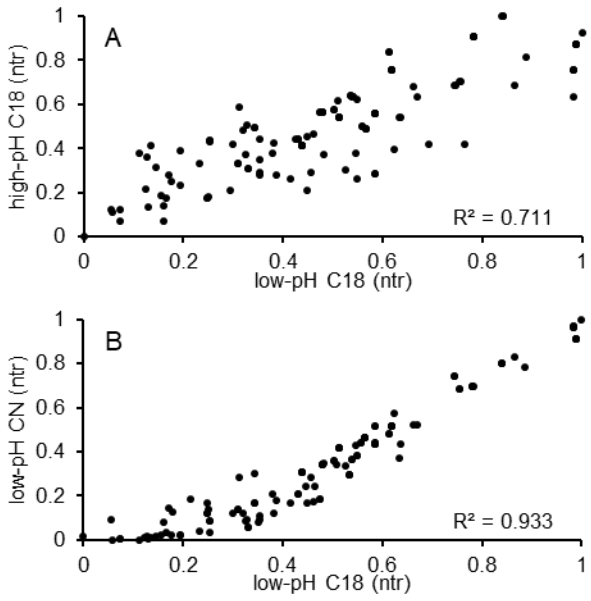

202

203 Figure 1: Orthogonality plots using normalized retention times (ntr) of targeted peptide
204 features. The following comparisons are presented: C18 using 0.1% FA (x-axis in all subplots)
205 vs HPH C18 using 20 mM AmFm at pH 10 (A), cyano using 0.1% FA (B).
206

207 ### *3.2 RPLC×RPLC method development: modulation and ^{1}D method*

208 The target of our method development was to establish a 60-min gradient time to realize
209 analysis with medium-throughput potentials. A modulation time of 30 seconds was chosen for
210 all 2DLC methods as it allows for frequent fractionation of the ^{1}D and running ^{2}D gradients
211 with high gradient volumes. Previous research on 2DLC parallel-gradients underlined the
212 negative effect of injection band broadening on the method's peak capacity when using passive
213 modulation (i.e. sampling loops where no analyte focussing takes place)[24]. Therefore, we
214 applied stationary-phase-assisted modulation (SPAM) as the modulation approach for the
215 2DLC methods. SPAM allowed diluting the ^{1}D eluent, facilitating anayte focussing on trap
216 columns before injection in ^{2}D gradients, reducing band broadening between separations. We
217 selected a 1:3 dilution ratio given the steep retention curves that peptides exhibit on C18
218 stationary phases (see SI Section S-7 Figure S4).

To develop the ^{1}D we opted for 0.16 mL min^{-1} as flow rate as a result of the Van Deemter curve analysis of the CN column (See SI Section S-7 Figure S5). We then tested linear gradients for the CN and HPH separations. The protein mixture digest was used as model sample for method development and evaluation purposes. The gradient slope was adjusted such that the peaks elute within 60 minutes, to spread the analytes as well as possible within the gradient time. The methods we selected for the HPH and CN columns used gradients from 2-38% and 2-32% ACN. Feature peak detection was performed on 146 masses (list and description are reported in SI files) and we obtained average full widths at half height (FWHM) of 0.121 min (HPH) and 0.172 min (CN) and a corresponding peak capacity of about 292 and 206 (tg = 60 min). In addition, an LPH method, which will be used as state-of-the-art 1DLC reference, was developed with a gradient from 2% to 38% B, resulting in peaks with an average FWHM of 0.120 min and a peak capacity of about 295.

3.2.1 Full and shifted-gradient RPLC×RPLC-HRMS methods

Full and shifted gradient methods were developed following principles discussed in recent 2DLC literature [4,14], coupling an HPH ^{1}D with LPH ^{2}D separation. We used high ^{2}D flow rates (1.4 mL min^{-1}) to increase the gradient volume and shorten the re-equilibration time for each ^{2}D separation. However, the maximum flow rate allowed from our ESI source was 0.7 mL min^{-1} and therefore we applied post-column 1:1 flow-split.

Figure 2A displays the results from the full-gradient RPLC×RPLC separation in the analysis of the protein mixture digest. This method presents a high correlation and, therefore, low 2DLC space utilization as can be observed by the clustering of the peaks. The results of the full-gradient measurements were used to design a shifted-gradient program, allowing us to extrapolate the upper and lower boundaries and times of the ^{2}D shifted gradient. Briefly, we

maintained the lower boundary of 6% B in the ^{2}D till 20 min, this was then increased linearly to 35% B till 60 min. The upper ^{2}D %B boundary started at 30% B and then increased linearly to 45% at 20 min and kept constant till the end of the run. Figure 2B presents the result of the analysis of the protein mixture digest by the shifted HPC×LPH method. The shifted-gradient programming significantly increased the utilization of the 2DLC space.

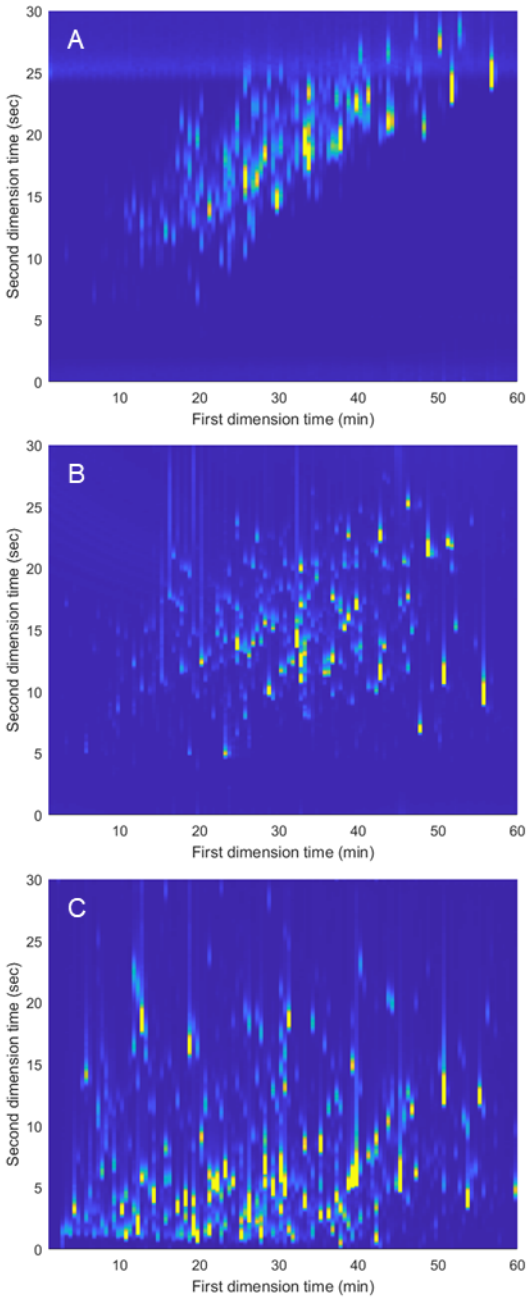

Figure 2: 2DLC plots of the BPC obtained from the protein-mixture digest sample using different gradient assemblies, full-gradient (A), shifted-gradient (B), and parallel-gradient (C).

In all plots, the intensity is represented by colour and scaled to a relative intensity such that all chromatograms appear equally visible despite absolute differences in peak heights. It should be noted for ease of visibility, the ^{2}D times in the Figure A, B have been shifted by 0.07 min and C by 0.24 min to account for dead time.

3.2.2 Parallel-gradient RPLC×RPLC-HRMS method

To develop the parallel-gradient, we selected the CN×LPH combination following what was described in section 3.1. The ^{1}D gradient method is described in section 3.2. The ^{1}D flow rate and modulation parameters were identical to the other methods. The ^{2}D flow rate was 0.7 mL min^{-1} allowing for splittless MS coupling (vs 1.4 mL min^{-1} of full and shifted-gradients). This was possible because in parallel-gradients RPLC×RPLC, there is no need for equilibration time between ^{2}D separations and it is not needed to deliver, in a short time, a gradient of several ^{2}D column volumes. This resulted in the inherent advantage of a reduced 2DLC dilution factor and avoiding flow splitting. However, broader ^{2}D peaks are expected from this gradient design due to the lower flow rate and shallow gradient elution conditions, resulting. Conversely, filling up the entire space without the need for column re-equilibration may increase the use of the separation space (surface coverage) and, therefore, the effective peak capacity.

For the 2D separation, a continuous gradient running in parallel to the ^{1}D gradient was developed. The ^{2}D gradient used a higher modifier percentage than the ^{1}D gradient, as higher retention was present in the LPH with respect to the CN method. Different offsets and slopes were tested to increase the spread of ^{2}D peaks over the modulation time while avoiding excessive retention to minimize excessive peak broadening. Finally, a ^{2}D gradient program running from 12% to 40% B was chosen. Figure 2C displays the obtained 2DLC chromatogram of the analysis of the protein mixture digest.

3.3 Comparison of the 2DLC separation methods

In this section, the performance of shifted and parallel-gradient methods will be compared in terms of (i) separation metrics, (ii) run-to-run repeatability and sensitivity, and (iii) data-dependent MS/MS protein identification analysis of a cell protein digest. In addition, in (iii), we will discuss the importance of the modulation time in parallel-gradients to increase protein and peptide metrics. Key data used for comparison are summarized in Table 1.

Table 1: Comparison of 1D and 2DLC methods for the analysis of protein digests extracting average data from detected features in terms of peak width, height, and area. In addition, data on surface coverage, effective peak capacity, and retention time repeatability (n=4) are reported.

Method	1D C18	Full	Shifted	Parallel
FWHM (min)	0.1212	0.0161	0.0129	0.0181
Height (counts)	2.23E+07	4.63E+06	1.26E+06	8.93E+06
Dilution Factor (2D)	N/A	288	232	162
Area (counts min)	1.51E+08	6.69E+08	9.02E+07	3.92E+08
SC	N/A	0.2613*	0.6226	0.7439
n'_c	292	263**	779**	757**
t_r rep. (s) (n=4)	N/A	N/A	0.2947	0.2877

* Only 100 features were used for the full-gradient as opposed to 300 for the other methods as significant peak overlap was observed. **Results obtained correcting for surface coverage (SC) and undersampling factor.

3.3.1 Effective peak capacities of shifted- and parallel-gradients

We evaluated the separation performance of the methods by calculating the effective peak capacity. This was obtained by combining the results of ^{1}D and ^{2}D peak capacity (^{1}D peak capacity data are discussed in 3.2), undersampling factor and 2DLC surface coverage analysis, following what described in. [31,32]

The ^{2}D peak capacity was calculated from the peak width from the feature detection analysis of 73 unique features having the highest peak height in shifted- and parallel-gradient methods. Broader peak widths (0.0181 parallel vs 0.0129 min shifted) were observed with parallel-gradients (see Figure S7). These results can be explained by the lower ^{2}D flow rate and the more limited gradient peak compression effects. Moreover, in parallel-gradients, analytes may have long retention times and possibly not elute within one modulation (wrap-around). The ^{2}D peak capacities of roughly 16 (parallel), 19.5 (shifted) per modulation were obtained.

To calculate the extent to which the ^{1}D peak capacity was kept due to the sampling frequency of our 2DLC methods we calculated the undersampling factor.[32] This factor was higher for shifted-gradients (4.56) respect to parallel-gradients (3.28) as the HPH separation had a higher peak capacity with respect to the CN.

Next, we investigated the use of the 2DLC separation space surface using the Convex Hull method[4,33,34]. This algorithm connects the outermost data points in a space with straight lines and computes the area of its inner surface. This surface area is then divided by the total available separation space to obtain a value between zero and one, where one represents full surface coverage (SC). In our study, to get the most fair comparison between the different gradient approaches, the complete 2D time was considered in all cases, and only the ^{1}D dead time (2 min) was omitted. Therefore, the total available space for all chromatograms was 58 minutes in the ^{1}D and 30 seconds in the ^{2}D. The SC was calculated using the peak tops of the 300 most abundant peaks (see SI Section S-7 Figure S6). The full-gradient method presented the lowest surface coverage with a value of about 0.26, shifted-gradient 0.62 and parallel-gradients the highest with 0.74. These results highlight the fraction of the 2D separation space that was unused (74, 38, and 26%, respectively) and, therefore, in which the MS detector was not analyzing analyte-related m/z features. The application of shifted-gradients clearly increased the usage of separation space. However, in each modulation the first 5

seconds were needed for column equilibration (16% of the total ^{2}D separation) and therefore not used for analysis. In the parallel-gradient method (Figure 2C), as no equilibration time was needed between runs, the analytes elute through almost the entire ^{2}D time. This resulted in a higher surface coverage, roughly 19% more than that obtained using a shifted-gradient program.

Finally, we calculated the effective peak capacity from the parameter described above (see SI Section S-5 for details) obtaining a value of 779 for the shifted-gradient and 757 for the parallel-gradient. The two methods provide similar separation performances, with the parallel gradient allowing for higher utilization of the 2DLC separation space (surface coverage) and the shifted gradients enabling sharper ^{2}D peaks. Parallel and shifted-gradients outperformed the full-gradient method and the 1D LPH method (peak capacity of 288 and 295 respectively).

3.3.2 Run-to-run repeatability and RPLC×RPLC-HRMS sensitivity

To achieve widespread implementation of LC×LC methods for routine use, the run-to-run repeatability is a crucial factor. To assess this, the shifted and parallel-gradient methods were subjected to four consecutive injections of the protein digest mixture and the variation in ^{2}D elution times between four runs was evaluated. Common features presented in all four measurements that eluted within one modulation were selected using the batch-pairing algorithm [35]. For the shifted-gradient method, the average standard deviation over the ^{2}D retention times was 0.2947 seconds, while for the parallel-gradient method, it was 0.2877 seconds. The distributions of the average retention time variation (n=4) for all these features are displayed in Figure S8 in SI Section S-7. We concluded that parallel and shifted gradient methods present similar deviations in ^{2}D retention times and can be considered sufficiently

repeatable as both averages were below 0.3 seconds, which was only several datapoints at the MS acquisition rate (between about 2 and 10 Hz).

Next, we investigated the difference in sensitivity of the methods, by applying feature detection and extracting peak area and heights. We observed a clear gain in sensitivity when using the parallel-gradient method, with about eight times higher average area ($8.94 \cdot 10^8$ vs. $1.26 \cdot 10^8$) and four times higher average peak height ($3.92 \cdot 10^8$ and $9.22 \cdot 10^7$). The difference observed was likely a result of the higher dilution factor in the shifted-gradients ^{2}D separation where the flow rate was double the one of the parallel-gradient (1.4 vs 0.7 mL min^{-1}). This was reflected in the higher calculated dilution factor (232 vs 162).

3.3.3 RPLC×RPLC-MS/MS of a cell lysate digest

Finally, tested if the increased separation power of the RPLC×RPLC methods developed yields higher protein identifications in the analysis of complex proteomics samples. To benchmark the methods' performance we applied the parallel, shifted-gradients and 1DLC LPH method to analyze the same amount of a complex protein digest (cell lysate (CL) of Human IMR90 lung fibroblast cells) in the same analysis time. This sample was selected as a representative sample for proteomics application with thousands of proteins present and subsequently digested.

Figure 3 displays the 2DLC chromatograms for shifted and parallel-gradient methods analysis of the CL. In both methods, significantly more peaks were visible than in the protein mixture digest used for method development. However, surface coverage, and peak width results were similar. A top 6 MS/MS data-dependent analysis was used to identify peptide sequences and infer the presence of proteins. Table 2 summarizes the results of the MS protein analysis (SI Section S-7 Table S9 for full details). We observed important differences in MS/MS results and peptide and protein identifications between the datasets. In particular, we observed in the 1D LPH method a higher ratio of MS/MS over full MS scans. This indicated that throughout

368 the analysis time five or more m/z features (not in the exclusion list dynamically changed every
369 20 seconds) and had intensity over the set threshold. In comparison, shifted and parallel-
370 gradients had lower ratios of about three. In the 1D LPH experiments, the peptides continuously
371 eluted from the column, with no gaps of analyte elution in the total ion chromatogram. This
372 was not the case for 2DLC measurements where gaps where no analytes eluted are present,
373 and, therefore, a lower number of MS/MS events took place. Moreover, 2DLC methods,
374 despite significantly increasing the peak capacity, may present lower sensitivity as a result of
375 the higher flow rates used in the ^{2}D separation and fractionation of ^{1}D peaks into multiple ^{2}D
376 separations. This is true in particular for shifted gradients were lower average MS intensity
377 with respect to the 1D LPH method (about 4 times less) were observed. We suggest that this is
378 the reason why the gains in separation obtained by both shifted and parallel-gradients do not
379 offer increased identification. In particular, shifted-gradients perform significantly worse than
380 the 1D LPH method, identifying about 80 and 45% less peptides and proteins. Instead, the
381 parallel-gradient methods gave results similar to the 1D LPH method with a comparable
382 number of proteins identified despite a lower number of peptides identified (33% less),
383 indicating that the 2DLC method may reduce the identification of peptides from the same
384 protein.

385 Following these results, we further developed the parallel-gradient method to improve
386 its LC-MS/MS performance. To achieve this, we decreased the modulation time to 20 and 10
387 seconds aiming to use wrap-around effects (analytes eluting after one modulation) to occupy
388 the less-used ^{2}D space in the second half of the initial modulation (SI Section S-7 Figures S9
389 and S10) and fill the gaps between modulations. However, this approach will (i) reduce the
390 peak capacity of the method as the lower modulation time will result in a lower peak capacity
391 per ^{2}D and (ii) will further increase the dilution of the method as ^{1}D peaks will be fractionated
392 in more ^{2}D separations (thus potentially reduce peak heights).

In our experiments, increasing the modulation frequency in parallel-gradients significantly increased the number of MS/MS events, reaching values similar to the one of 1D LPH (ratio MS/MS to MS of 5), demonstrating that distributing the analytes within the ^{2}D separation and reducing the gaps analytes elution gaps beween modulations has a significant effect in the analysis of highly complicated samples. The best results in terms of protein analysis from 2DLC experiments were achieved using 10 seconds modulations with an increase of peptides (12 %) and proteins (22%) identified respect to 1D LPH. Interestingly, these results were achieved despite reducing the calculated 2DLC effective peak capacity (706 and 564 using 20 and 10 sec modulation times).

Table 2: Number of MS and MS/MS events observed in the 1D and 2DLC-HRMS dataset in the elution area between 2 and 60 min and the related peptide and protein identifications.

Method	MS/MS	Ratio MS/MS to MS	Average MS intensity	Peptide IDs	Protein IDs
1D-C18 1	25568	5.27	9.43E+06	5858	1539
1D-C18 2	26198	5.49	1.10E+07	6275	1554
Shift 1	19312	3.29	2.71E+06	2670	977
Shift 2	19157	3.25	2.17E+06	2565	967
Parallel 30s 1	20780	3.60	1.43E+07	4142	1539
Parallel 30s 2	21106	3.69	1.42E+07	3774	1554
Parallel 20s 1	24425	4.73	1.23E+07	5420	1786
Parallel 20s 2	24484	4.77	1.15E+07	5086	1730
Parallel 10s 1	26262	5.37	1.44E+07	7177	1994
Parallel 10s 2	26170	5.36	1.47E+07	7144	1989

*data considered are between 2 and 60 min.

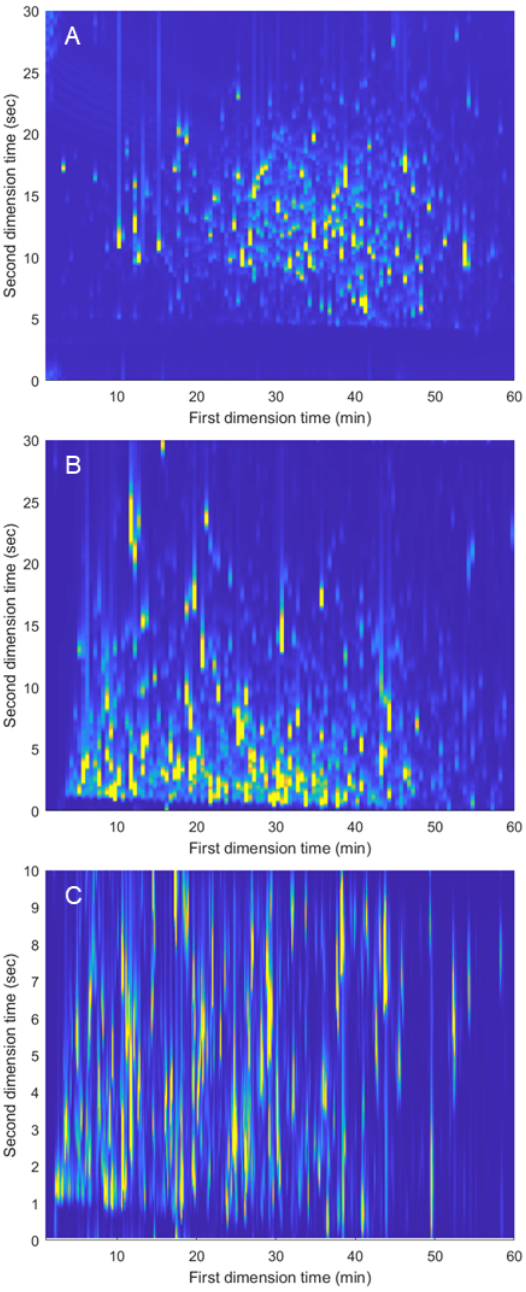

407

408 Figure 3: Base-peak RPLC×RPLC-MS/MS chromatograms of a cell lystate of human IMR90
409 lung fibroblast cells using the shifted-gradient method (A) and the parallel-gradient method
410 using 30-second modulations (B) and 10-second modulations (C).
411

4. Conclusions

This study compared the use of shifted and parallel-gradients designs for the second dimension in correlated LC×LC separations. Shifted gradients can achieve the highest effective peak capacities and the narrowest peak widths. They also achieve significantly better surface coverage than conventional full-gradient approaches. However, to achieve high peak capacity ^{2}D separations, high flow rates have to be used, reducing the MS sensitivity. Moreover, part of the separation space is solely used for ^{2}D column re-equilibration, introducing gaps in the MS/MS analysis.

Parallel-gradient provide lower effective peak capacity but have higher 2DLC surface coverage and sensitivity. Furthermore, this approach had a lower solvent consumption (35.7 mL and 19.5 mL per run for shifted and parallel-gradients, respectively). Most importantly, in analyzing highly complex protein digests by MS/MS, parallel-gradients obtained significantly higher protein identification numbers than the shifted-gradient method. Moreover, reducing the modulation time (here to 10 seconds) allowed to exploit wrap-around effects, allowing to more evenly distribute the analytes within each modulation.

In future studies, it may be valuable to consider these shorter modulation times for parallel-gradient designs in RPLC×RPLC. Moreover, MS instrumentation with higher MS and MS/MS frequencies and data acquisition strategies such as MS/MS data-independent-analysis may be able to take even greater advantage of the extra separation power offered by LC×LC compared with that of 1D separations. Automated method development may aid in simplifying the design of both shifted and parallel gradient designs and may further improve the overall performance of such methods. Lastly, it should be repeated that striving for maximal peak capacity or surface coverage will not always contribute to the goal of the analytical method, and therefore the metric used to describe the performance of the separation should carefully be selected.

Associated content

Supporting Information:

Details regarding the sample preparation, instrumental settings, data processing protocols, several figures displaying additional experimental data and CRediT authorship contribution statement.

Notes

The authors declare no competing financial interest.

Acknowledgments

RH Acknowledges the PARADISE project (ENPPS.TA.019.001) and received funding from the Dutch Research Council (NWO) in the framework of the Science PPP Fund for the top sectors and from the Ministry of Economic Affairs of the Netherlands in the framework of the "PPS Toeslagregeling". Stef Molenaar is acknowledged for his assistance with the batch-pairing algorithm used for peak pairing data used for the run-to-run repeatability evaluation. Ziran Zhai is acknowledged for his assistance setting up the MS measurements.

References

(1) Drabovich, A. P.; Pavlou, M. P.; Batruch, I.; Diamandis, E. P. Proteomic and Mass Spectrometry Technologies for Biomarker Discovery. In *Proteomic and Metabolomic Approaches to Biomarker Discovery*; Elsevier, 2013; pp 17–37. https://doi.org/10.1016/B978-0-12-394446-7.00002-9.

(2) Dupree, E. J.; Jayathirtha, M.; Yorkey, H.; Mihasan, M.; Petre, B. A.; Darie, C. C. A Critical Review of Bottom-Up Proteomics: The Good, the Bad, and the Future of This Field. *Proteomes* **2020**, *8* (3), 14. https://doi.org/10.3390/proteomes8030014.

(3) Shuken, S. R. An Introduction to Mass Spectrometry-Based Proteomics. *J Proteome Res* **2023**. https://doi.org/10.1021/acs.jproteome.2c00838.

(4) Stoll, D. R.; Lhotka, H. R.; Harmes, D. C.; Madigan, B.; Hsiao, J. J.; Staples, G. O. High Resolution Two-Dimensional Liquid Chromatography Coupled with Mass Spectrometry for Robust and Sensitive Characterization of Therapeutic Antibodies at the Peptide Level. *J Chromatogr B Analyt Technol Biomed Life Sci* **2019**, *1134–1135* (August), 121832. https://doi.org/10.1016/j.jchromb.2019.121832.

(5) Shishkova, E.; Hebert, A. S.; Coon, J. J. Now, More Than Ever, Proteomics Needs Better Chromatography. *Cell Syst* **2016**, *3* (4), 321–324. https://doi.org/10.1016/j.cels.2016.10.007.

(6) Giddings, J. Calvin. Maximum Number of Components Resolvable by Gel Filtration and Other Elution Chromatographic Methods. *Anal Chem* **1967**, *39* (8), 1027–1028. https://doi.org/10.1021/ac60252a025.

(7) Köcher, T.; Swart, R.; Mechtler, K. Reveals a Linear Relation between Peak Capacity and Number. *Anal Chem* **2011**, *83* (7), 2699–2704. https://doi.org/10.1021/ac103243t.

(8) Pirok, B. W. J.; Stoll, D. R.; Schoenmakers, P. J. Recent Developments in Two-Dimensional Liquid Chromatography: Fundamental Improvements for Practical Applications. *Anal Chem* **2019**, *91* (1), 240–263. https://doi.org/10.1021/acs.analchem.8b04841.

(9) Pirok, B. W. J.; Gargano, A. F. G.; Schoenmakers, P. J. Optimizing Separations in Online Comprehensive Two-Dimensional Liquid Chromatography. *J Sep Sci* **2018**, *41* (1), 68–98. https://doi.org/10.1002/jssc.201700863.

(10) Stoll, D. R.; Carr, P. W. Two-Dimensional Liquid Chromatography: A State of the Art Tutorial. *Anal Chem* **2017**, *89* (1), 519–531. https://doi.org/10.1021/acs.analchem.6b03506.

(11) Pirok, B. W. J.; Schoenmakers, P. J. Practical Approaches to Overcome the Challenges of Comprehensive Two-Dimensional Liquid Chromatography. *LCGC Europe* **2018**, *31* (5), 242–249.

(12) van den Hurk, R. S.; Pursch, M.; Stoll, D. R.; Pirok, B. W. J. Recent Trends in Two-Dimensional Liquid Chromatography. *Trends in Analytical Chemistry* **2023**, 117166. https://doi.org/10.1016/j.trac.2023.117166.

(13) Sarrut, M.; Rouvière, F.; Heinisch, S. Theoretical and Experimental Comparison of One Dimensional versus On-Line Comprehensive Two Dimensional Liquid Chromatography for Optimized Sub-Hour Separations of Complex Peptide Samples. *J Chromatogr A* **2017**, *1498*, 183–195. https://doi.org/10.1016/j.chroma.2017.01.054.

(14) Chapel, S.; Rouvière, F.; Heinisch, S. Sense and Nonsense of Shifting Gradients in On-Line Comprehensive Reversed-Phase LC × Reversed-Phase LC. *J Chromatogr B Analyt Technol Biomed Life Sci* **2022**, *1212* (August). https://doi.org/10.1016/j.jchromb.2022.123512.

(15) Gunnarson, C.; Lauer, T.; Willenbring, H.; Larson, E.; Dittmann, M.; Broeckhoven, K.; Stoll, D. R. Implications of Dispersion in Connecting Capillaries for Separation Systems Involving Post-Column Flow Splitting. *J Chromatogr A* **2021**, *1639*. https://doi.org/10.1016/j.chroma.2021.461893.

(16) Venkatramani, C. J.; Zelechonok, Y. An Automated Orthogonal Two-Dimensional Liquid Chromatograph. *Anal Chem* **2003**, *75* (14), 3484–3494. https://doi.org/10.1021/ac030075w.

(17) Jandera, P.; Česla, P.; Hájek, T.; Vohralík, G.; Vyňuchalová, K.; Fischer, J.; ??esla, P.; H??jek, T.; Vohral??k, G.; Vy??uchalov??, K.; Fischer, J. Optimization of Separation in Two-Dimensional High-Performance Liquid Chromatography by Adjusting Phase System Selectivity and Using Programmed Elution Techniques. *J Chromatogr A* **2008**, *1189* (1–2), 207–220. https://doi.org/10.1016/j.chroma.2007.11.053.

(18) Česla, P.; Hájek, T.; Jandera, P. Optimization of Two-Dimensional Gradient Liquid Chromatography Separations. *J Chromatogr A* **2009**, *1216* (16), 3443–3457. https://doi.org/10.1016/j.chroma.2008.08.111.

(19) Cacciola, F.; Jandera, P.; Hajdú, Z.; Česla, P.; Mondello, L. Comprehensive Two-Dimensional Liquid Chromatography with Parallel Gradients for Separation of Phenolic and Flavone Antioxidants. *J Chromatogr A* **2007**, *1149* (1), 73–87. https://doi.org/10.1016/j.chroma.2007.01.119.

(20) Aly, A. A.; Muller, M.; de Villiers, A.; Pirok, B. W. J.; Górecki, T. Parallel Gradients in Comprehensive Multidimensional Liquid Chromatography Enhance Utilization of the Separation Space and the Degree of Orthogonality When the Separation Mechanisms Are Correlated. *J Chromatogr A* **2020**, *1628*, 461452. https://doi.org/10.1016/j.chroma.2020.461452.

(21) Shoykhet, K.; Stoll, D.; Buckenmaier, S. Constant Pressure Mode of Operation in the Second Dimension of Two-Dimensional Liquid Chromatography: A Proof of Concept. *J Chromatogr A* **2021**, *1639*, 461880. https://doi.org/10.1016/j.chroma.2021.461880.

(22) Aly, A. A.; Muller, M.; de Villiers, A.; Pirok, B. W. J.; Górecki, T. Parallel Gradients in Comprehensive Multidimensional Liquid Chromatography Enhance Utilization of the Separation Space and the Degree of Orthogonality When the Separation Mechanisms Are Correlated. *J Chromatogr A* **2020**, *1628*, 461452. https://doi.org/10.1016/j.chroma.2020.461452.

(23) Byrdwell, W. C.; Kotapati, H. K.; Goldschmidt, R.; Jakubec, P.; Nováková, L. Three-Dimensional Liquid Chromatography with Parallel Second Dimensions and Quadruple Parallel Mass Spectrometry for Adult/Infant Formula Analysis. *J Chromatogr A* **2022**, *1661*, 462682. https://doi.org/10.1016/j.chroma.2021.462682.

(24) Cacciola, F.; Jandera, P.; Hajdú, Z.; Česla, P.; Mondello, L. Comprehensive Two-Dimensional Liquid Chromatography with Parallel Gradients for Separation of Phenolic and Flavone Antioxidants. *J Chromatogr A* **2007**, *1149* (1), 73–87. https://doi.org/10.1016/j.chroma.2007.01.119.

(25) Vonk, R. J.; Gargano, A. F. G.; Davydova, E.; Dekker, H. L.; Eeltink, S.; de Koning, L. J.; Schoenmakers, P. J. Comprehensive Two-Dimensional Liquid Chromatography with Stationary-Phase-Assisted Modulation Coupled to High-Resolution Mass Spectrometry Applied to Proteome Analysis of Saccharomyces Cerevisiae. *Anal Chem* **2015**, *87* (10), 5387–5394. https://doi.org/10.1021/acs.analchem.5b00708.

(26) Gargano, A. F. G.; Duffin, M.; Navarro, P.; Schoenmakers, P. J. Reducing Dilution and Analysis Time in Online Comprehensive Two-Dimensional Liquid Chromatography by Active Modulation. *Anal Chem* **2016**, *1*, 1–16. https://doi.org/10.1021/acs.analchem.5b04051.

(27) Baglai, A.; Blokland, M. H.; Mol, H. G. J.; Gargano, A. F. G.; van der Wal, S.; Schoenmakers, P. J. Enhancing Detectability of Anabolic-Steroid Residues in Bovine Urine by Actively Modulated Online Comprehensive Two-Dimensional Liquid Chromatography - High-Resolution Mass Spectrometry. *Anal Chim Acta* **2018**, *1013*, 87–97. https://doi.org/10.1016/j.aca.2017.12.043.

(28) Doubleday, P. F.; Fornelli, L.; Kelleher, N. L. Elucidating Proteoform Dynamics Underlying the Senescence Associated Secretory Phenotype. *J Proteome Res* **2020**, *19*, 938–948. https://doi.org/10.1021/acs.jproteome.9b00739.

(29) Roca, L. S.; Schoemaker, S. E.; Pirok, B. W. J.; Gargano, A. F. G.; Schoenmakers, P. J. Accurate Modelling of the Retention Behaviour of Peptides in Gradient-Elution Hydrophilic Interaction Liquid Chromatography. *J Chromatogr A* **2020**, *1614*, 460650. https://doi.org/10.1016/j.chroma.2019.460650.

(30) Schmid, R.; Heuckeroth, S.; Korf, A.; Smirnov, A.; Myers, O.; Dyrlund, T. S.; Bushuiev, R.; Murray, K. J.; Hoffmann, N.; Lu, M.; Sarvepalli, A.; Zhang, Z.; Fleischauer, M.; Dührkop, K.; Wesner, M.; Hoogstra, S. J.; Rudt, E.; Mokshyna, O.; Brungs, C.; Ponomarov, K.; Mutabdžija, L.; Damiani, T.; Pudney, C. J.; Earll, M.; Helmer, P. O.; Fallon, T. R.; Schulze, T.; Rivas-Ubach, A.; Bilbao, A.; Richter, H.; Nothias, L. F.; Wang, M.; Orešič, M.; Weng, J. K.; Böcker, S.; Jeibmann, A.; Hayen, H.; Karst, U.; Dorrestein, P. C.; Petras, D.; Du, X.; Pluskal, T. Integrative Analysis of Multimodal Mass Spectrometry Data in MZmine 3. *Nat Biotechnol* **2023**, *41* (4), 447–449. https://doi.org/10.1038/s41587-023-01690-2.

(31) Stoll, D. R.; Wang, X.; Carr, P. W. Comparison of the Practical Resolving Power of One- and Two-Dimensional High-Performance Liquid Chromatography Analysis of Metabolomic Samples. *Anal Chem* **2008**, *80* (1), 268–278. https://doi.org/10.1021/ac701676b.

(32) Davis, J. M.; Stoll, D. R.; Carr, P. W. Dependence of Effective Peak Capacity in Comprehensive Two-Dimensional Separations on the Distribution of Peak Capacity between the Two Dimensions. *Anal Chem* **2008**, *80* (21), 8122–8134. https://doi.org/10.1021/ac800933z.

(33) Semard, G.; Peulon-Agasse, V.; Bruchet, A.; Bouillon, J. P.; Cardinaël, P. Convex Hull: A New Method to Determine the Separation Space Used and to Optimize Operating Conditions for Comprehensive Two-Dimensional Gas Chromatography. *J*

Chromatogr A **2010**, *1217* (33), 5449–5454.
https://doi.org/10.1016/j.chroma.2010.06.048.

(34) Aly, A. A.; Muller, M.; de Villiers, A.; Pirok, B. W. J.; Górecki, T. Parallel Gradients in Comprehensive Multidimensional Liquid Chromatography Enhance Utilization of the Separation Space and the Degree of Orthogonality When the Separation Mechanisms Are Correlated. *J Chromatogr A* **2020**, *1628*, 461452. https://doi.org/10.1016/j.chroma.2020.461452.

(35) Molenaar, S. R. A.; Mommers, J. H. M.; Stoll, D. R.; Ngxangxa, S.; de Villiers, A. J.; Schoenmakers, P. J.; Pirok, B. W. J. Algorithm for Tracking Peaks amongst Numerous Datasets in Comprehensive Two-Dimensional Chromatography to Enhance Data Analysis and Interpretation. *J Chromatogr A* **2023**, *1705* (March). https://doi.org/10.1016/j.chroma.2023.464223.

595 Figure for table of contents only

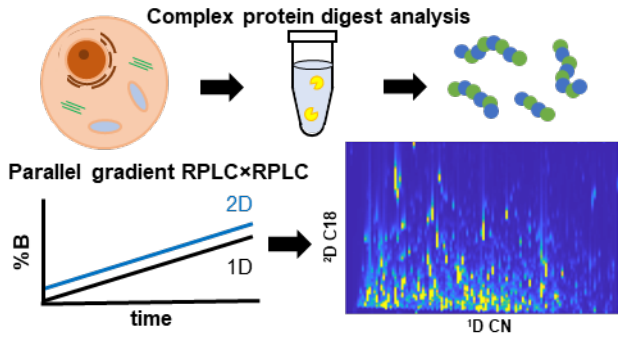

596